Calculation of electron-impact ionization using the J-matrix method

D. A. Konovalov
Discipline of Information Technology, School of Business, James Cook University, Townsville, Queensland 4811, Australia

I. Bray
ARC Centre for Antimatter-Matter Studies, Curtin University of Technology, GPO Box U1987, Perth, Western Australia 6845, Australia

(Received 24 May 2010; published 13 August 2010)

The J-matrix approach to electron-atom scattering is applied to ionization processes. We consider the Temkin-Poet model of e-H ionization. Convergence issues are studied with greater detail than previously possible using other close-coupling methods. The numerical strengths of the technique are emphasized with the long-term goal of application to ionization-plus-excitation processes.

DOI: 10.1103/PhysRevA.82.022708 PACS number(s): 34.80.Dp

I. INTRODUCTION

The J-matrix (JM) method is a theoretical framework for solving a quantum scattering problem using only square-integrable (L^2) basis functions [1,2]. When initially applied to the s-wave electron-atomic-hydrogen scattering problem, the method exhibited the so-called pseudoresonances [3], which have always been the main objection against L^2-based methods. However, arguably, the pseudoresonances are not an issue provided they disappear from the physical observables as the size of a particular L^2 basis increases [4,5]. Such convergence has now been demonstrated for the JM method by calculating elastic and a number of excitation cross sections for electron scattering on hydrogen (e-H) [6,7] and helium (e-He) [8]. Furthermore, the JM results were found to be in agreement [9] with other *ab initio* scattering approaches such as the convergent-close-coupling (CCC) [5] and the intermediate energy R-matrix (IERM) [10] methods. Since the JM method continues to be actively explored [11–17], it is interesting to revisit the JM method paying particular attention to its rate of convergence, which is the first objective of this study.

The second goal of this study is to apply the JM method to the ionization phenomena for the first time. The s-wave electron-hydrogen scattering problem, that is, the Temkin-Poet problem [18,19], was used as a relevant scattering benchmark problem [7,20–22] to demonstrate the results.

Arguably, the main and the only concern of an L^2-based scattering method is, or at least should be, the convergence rate to the exact solution as the number L^2 basis functions increases [23]. Since such convergence verifications could be computationally intensive, a new variable transformation was designed to optimize the required numerical integrations.

More broadly, our goal is to develop the JM approach to a generally applicable collision theory that combines the strengths of the R-matrix approach, specifically, upon solution the results are available for a broad range of incident energies, and the CCC method, where convergence is systematically approached by simply increasing the L^2 basis size. Ultimately, the L^2 description of the total wave function should make it possible to develop an iterative close-coupling formulation, where the JM solution of say e-He^+ scattering would form the wave functions to be used in the close-coupling expansion of e-He scattering. These wave functions would have the correct channel information and allow such calculations to directly yield ionization-plus-excitation cross sections. Having stated our long-term objectives, we first need to demonstrate the utility of the JM approach, and this is why we begin with the Temkin-Poet model.

The presented JM results are calculated using Java programming language which is freely available for MS Windows, Mac OSX, and some versions of Linux/Unix. The complete Java source code used in this study is freely available from jmatrix.googlecode.com or a relevant link at www.dmitrykonovalov.org for academic use.

II. THEORY

A. Potential scattering

This subsection summarizes the JM formalism on the example of nonrelativistic s-scattering of one electron in a short-range central symmetric potential field $V(r)$, for example, one created by the ground state of the hydrogen atom $V_{1s}(r) = (1 + 1/r)\exp(-2r)$ [24], where the atomic units are used throughout this study. After the partial-wave expansion and retaining only the s terms ($l = 0$), the potential scattering problem is reduced [24,25] to solving the radial Schrödinger equation,

$$(H - E)\Psi(r) = 0, \tag{1}$$

$$\Psi(r \to \infty) \sim \sin(kr + \delta), \quad \Psi(0) = 0, \tag{2}$$

$$H = K + V(r), \quad K = -\frac{1}{2}\frac{d^2}{dr^2}, \tag{3}$$

where δ is the phase shift and $E = k^2/2$ is the total energy of the system.

The JM formalism [1,26] requires a set of real L^2 tridiagonal (or diagonal) basis functions, $\{|\phi_n\rangle\}_{n=0}^{\infty}$, such that $\phi_n(0) = 0$ and $(K - E)$'s matrix is tridiagonal,

$$J_{nm} = \langle\phi_n|K - E|\phi_m\rangle = 0, \quad |n - m| > 1, \tag{4}$$

$$\langle\phi_n|\phi_m\rangle = 0, \quad |n - m| > 1. \tag{5}$$

To achieve a uniform treatment of both potential and multichannel scattering, an additional basis of N orthonormal functions $\{|\chi_n\rangle\}_{n=0}^{N-1}$ is defined as linear combinations of the

 ©2010 The American Physical Society

first N JM basis functions,

$$\chi_n(r) = \sum_{m=0}^{N-1} D_{nm}\phi_m(r). \tag{6}$$

For the potential scattering, such orthonormal basis could be constructed from the diagonalization of the system's Hamiltonian,

$$\langle\chi_n|H|\chi_m\rangle = e_n\delta_{nm}, \quad \langle\chi_n|\chi_m\rangle = \delta_{nm}. \tag{7}$$

Closely following Broad and Reinhardt [2] except for the use of the orthonormal basis, $\Psi(r)$ is approximated by $\Psi^N(r)$,

$$\Psi(r) \approx \Psi^N(r) = \sum_{m=0}^{N-1} \chi_m(r)a_m + \sum_{p=N}^{\infty} \phi_p(r)f_p, \tag{8}$$

$$f_p = s_p + Rc_p, \tag{9}$$

where a_m are the *inner*-space expansion coefficients describing the electron's interaction with $V(r)$ and $R = \tan\delta$ is the s term of the reactance matrix (also known as the K matrix [25]). The second sum in (8) is the *outer*-space part describing a free moving electron in terms of the regular or sinelike (s_p coefficients) and irregular or cosinelike (c_p coefficients) solutions of

$$\sum_{p=0}^{\infty} J_{np}s_p = 0, \quad \sum_{p=0}^{\infty} J_{np}c_p = w\delta_{n,0}, \tag{10}$$

with a uniquely defined constant w. The unknown a_m and R are found by simultaneously solving

$$\langle\chi_n|H - E|\Psi^N\rangle = 0, \quad n < N, \tag{11}$$

$$\langle\phi_n|H - E|\Psi^N\rangle = 0, \quad n \geqslant N. \tag{12}$$

Note that Eqs. (10) are central to the JM formalism as they could be solved analytically for some types of the basis functions [15]. To take advantage of the analytical solutions for s_n and c_n, the representation of $V(r)$ in the chosen basis is truncated to an $N \times N$ matrix by retaining only the inner functional-space contributions,

$$V_{nm} \approx V^N_{nm} = \begin{cases} \langle\phi_n|V|\phi_m\rangle & \text{if } n,m < N \\ 0 & \text{otherwise,} \end{cases} \tag{13}$$

obtaining

$$\langle\chi_n|H - E|\phi_p\rangle \approx \langle\chi_n|K - E|\phi_p\rangle, \quad n < N,\ p \geqslant N, \tag{14}$$

$$\langle\phi_p|H - E|\phi_{p'}\rangle \approx J_{pp'}, \quad p,p' \geqslant N. \tag{15}$$

By this neglecting V_{nm} in the outer functional space, Eqs. (11) and (12) are reduced to the following three cases:

$$(e_n - E)a_n = -D_{n,N-1}J_{N-1,N}f_N, \quad n < N, \tag{16}$$

$$\sum_{m=0}^{N-1} D_{m,N-1}a_m = f_{N-1}, \quad n = N, \tag{17}$$

$$\sum_{p=N}^{\infty} J_{np}f_p = 0, \quad n > N, \tag{18}$$

where (18) is automatically satisfied via (10) and

$$J_{NN}f_N + J_{N,N+1}f_{N+1} = -J_{N,N-1}f_{N-1} \tag{19}$$

was used in (17).

Note that while the original JM formulation used $\phi_m(r)$ instead of $\chi_m(r)$ in (8), the final expression for R remains the same, completing the JM treatment of the potential scattering,

$$R = -(WCJC)^{-1}(WSJS), \tag{20}$$

where the s-wave partial S matrix and elastic cross section are given by

$$S_{00} = (1 + iR)(1 - iR)^{-1}, \tag{21}$$

$$\sigma_{00} = \frac{\pi}{k^2}|S_{00} - 1|^2, \tag{22}$$

respectively, and where

$$(WSJS) = Ws_NJ_{N,N-1} + s_{N-1}, \tag{23}$$

$$(WCJC) = Wc_NJ_{N,N-1} + c_{N-1}, \tag{24}$$

$$W = \sum_{m=0}^{N-1} \frac{D^2_{m,N-1}}{e_m - E}. \tag{25}$$

B. Multichannel scattering

The focus of this study is the Temkin-Poet model [18,19] of electron-atomic-hydrogen nonrelativistic collision with zero total angular momentum for two electrons,

$$(H - E)\Psi(r_1,r_2) = 0, \tag{26}$$

$$H = H_t + K_2 + V(r_1,r_2), \tag{27}$$

$$H_t = K_1 - \frac{1}{r_1}, \quad V(r_1,r_2) = -\frac{1}{r_2} + \frac{1}{\max(r_1,r_2)}, \tag{28}$$

where $\Psi(r_1,r_2) = (-1)^S\Psi(r_2,r_1)$ is symmetric for the singlet (total spin $S = 0$) and antisymmetric for triplet $S = 1$ scattering.

While the use of the system's eigenvectors in the JM expansion of $\Psi(r)$ (8) yields, arguably, a simpler set of equations for a_m and R, the main advantage of this approach lies in it being naturally extendable to the multichannel scattering, as shown in what follows.

An interesting clarification is now required before JM is generalized to the multichannel case. The purpose of the JM method is to solve a scattering problem rather than the electronic structure of the target or the target-electron systems. Therefore, the target states must be orthogonal to the outer JM basis functions, $\{|\phi_n\rangle\}_{n=N}^{\infty}$, to avoid interfering with the JM scattering equations. Keeping this in mind and following the approach outlined in the potential scattering, an orthonormal basis is created from the first N JM basis functions (6) via the following two-step procedure.

The first step ensures that any target state is orthogonal to the outer JM functions, $\{|\phi_n\rangle\}_{n=N}^{\infty}$. This is always true if the first $N_t < N$ orthonormal functions, $\{|\chi_\alpha\rangle\}_{\alpha=0}^{N_t-1}$, are created by diagonalizing the target Hamiltonian on the subset of only the first N_t JM basis functions,

$$\langle\chi_\alpha|H_t|\chi_\beta\rangle = e_\alpha\delta_{\alpha\beta}, \quad \langle\chi_\alpha|\chi_\beta\rangle = \delta_{\alpha\beta}, \tag{29}$$

$$\chi_\alpha(r) = \sum_{m=0}^{N_t-1} d_{\alpha m}\phi_m(r). \tag{30}$$

Hereafter the Greek indices will be assumed to vary between zero and $N_t - 1$, for example, $0 \leqslant \alpha,\beta < N_t$.

In the second step, the remaining $N - N_t$ orthonormal basis function is constructed from all first N JM functions, for example,

$$\chi_{N-1}(r) = \sum_{m=0}^{N-1} d_{N-1,m}\phi_m(r), \tag{31}$$

such that $\langle\chi_n|\chi_m\rangle = \delta_{n,m}$, $0 \leqslant n,m < N$. Equations (30) and (31) could be combined into a single expression (6), where

$$D_{nm} = \begin{cases} 0 & \text{if } n < N_t \text{ and } m \geqslant N_t \\ d_{nm} & \text{otherwise.} \end{cases} \tag{32}$$

If the lowest-energy target eigenvector $\chi_0(r)$ describes the ground target state exactly or with sufficient accuracy and considering only the case with the target hydrogen atom being in its ground state before the collision, the total energy of the system is given by

$$E = e_0 + E_0, \quad E_0 = k_0^2/2. \tag{33}$$

Using $\{|\chi_n\rangle\}_{n=0}^{N-1}$ as the one-electron basis, the two-electron basis could be constructed for the inner JM functional space via

$$\Phi_{\beta m}(r_1,r_2) = \hat{A}_{\beta m}\chi_\beta(r_1)\chi_m(r_2), \tag{34}$$

where $0 \leqslant \beta < N_t$ and $0 \leqslant m < N$ such that $\beta \leqslant m$ for $S = 0$ and $\beta < m$ for $S = 1$, and where $\hat{A}$ is the symmetrization operator defined from the coordinate space exchange operator $\hat{P}_r$ via

$$\hat{A}_{nm}|\chi_n\chi_m\rangle = b_{nm}[1 + (-1)^S\hat{P}_r]|\chi_n\chi_m\rangle, \tag{35}$$

with the normalization constant $b_{nm} = \frac{1}{2}$ for $n = m$ and $b_{nm} = \frac{1}{\sqrt{2}}$ for $n \neq m$. The system's eigenvectors are then obtained by diagonalizing H using all available two-electron configurations,

$$\langle\xi_i|H|\xi_j\rangle = E_i\delta_{ij}, \quad \langle\xi_i|\xi_j\rangle = \delta_{ij}, \tag{36}$$

$$\xi_i(r_1,r_2) = \sum_{\beta'=0}^{N_t-1}\sum_{m=\beta'}^{N-1} C_{i,\beta'm}\Phi_{\beta'm}(r_1,r_2). \tag{37}$$

Extending the preceding JM approach from the potential scattering to the multichannel scattering and following Broad and Reinhardt [2] whenever possible, $\Psi(r_1,r_2)$ is approximated by $\Psi^N(r_1,r_2)$ for the given total energy E,

$$\Psi^N = \sum_j \xi_j a_j + \sum_{\alpha=0}^{N_t-1}\sum_{p=N}^{\infty}\hat{A}_{\alpha p}\chi_\alpha(r_1)\phi_p(r_2)f_p^{\alpha\beta}, \tag{38}$$

$$f_p^{\alpha\beta} = \left(s_p^\alpha\delta_{\alpha\beta} + c_p^\alpha R_{\alpha\beta}\right)/\sqrt{k_\alpha}, \tag{39}$$

where $k_\alpha = \sqrt{2|E - e_\alpha|}$. The *open* channels are defined by $(E - e_\alpha) > 0$, while for the *closed* channels, $(E - e_\alpha) \leqslant 0$, $s_p^\alpha = 0$, and c_p^α is replaced by $(s_p^\alpha + ic_p^\alpha)$ evaluated at $q_\alpha = ik_\alpha$. The index of the incident channel β is defined only for the open channels in Eqs. (38) and (39), $0 \leqslant \beta < N_E$, where N_E is the number of open channels, $1 \leqslant N_E \leqslant N_t$.

Similar to (11) and (12), the a_j and $R_{\alpha\beta}$ coefficients are found by simultaneously solving the following equations for the inner and outer functional space, respectively,

$$\langle\xi_i|H - E|\Psi^N\rangle = 0, \tag{40}$$

$$\langle\hat{A}\chi_{\alpha'}(r_1)\phi_{p'}(r_2)|H - E|\Psi^N\rangle = 0, \quad p' \geqslant N. \tag{41}$$

As before, the target-projectile interaction matrix elements involving outer JM functions are ignored; that is, $\langle\phi_n\phi_p|V|\phi_m\phi_{p'}\rangle = 0$ when $p \geqslant N$ or $p' \geqslant N$, obtaining

$$\langle\chi_\alpha\chi_m|H - E|\chi_\beta\phi_p\rangle \approx \delta_{\alpha\beta}\delta_{pN}J_{N-1,N}^\beta D_{m,N-1}, \tag{42}$$

$$\langle\chi_m\chi_\alpha|H - E|\chi_\beta\phi_p\rangle \approx 0, \tag{43}$$

where $J_{nm}^\beta = \langle\phi_n|K - (E - e_\beta)|\phi_m\rangle$.

After some algebra, the final set of JM multichannel equations becomes

$$(E_i - E)a_i = -\sum_{\alpha=0}^{N-1} X_i^\alpha J_{N-1,N}^\alpha f_N^{\alpha\beta}, \tag{44}$$

$$\sum_j X_j^{\alpha'}a_j = f_{N-1}^{\alpha'\beta}, \tag{45}$$

$$X_i^\alpha = \sum_{m=N_t}^{N-1} C_{i,\alpha m}D_{m,N-1}, \tag{46}$$

and after elimination of a_i

$$\sum_{\alpha=0}^{N_t-1} W_{\alpha'\alpha}J_{N-1,N}^\alpha f_N^{\alpha\beta} = -f_{N-1}^{\alpha'\beta}, \tag{47}$$

$$W_{\alpha'\alpha} = \sum_j \frac{X_j^{\alpha'}X_j^\alpha}{E_j - E}. \tag{48}$$

Solving (47) for the reactance matrix yields

$$R_{\alpha\beta} = -\sum_{\alpha'=0}^{N_t-1}(WCJC)_{\alpha\alpha'}^{-1}(WSJS)_{\alpha'\beta}, \tag{49}$$

where $0 \leqslant \beta < N_E$,

$$(WSJS)_{\alpha'\beta} = \left(W_{\alpha'\beta}J_{N,N-1}^\beta s_N^\beta + \delta_{\alpha'\beta}s_{N-1}^\beta\right)/\sqrt{k_\beta}, \tag{50}$$

$$(WCJC)_{\alpha'\alpha} = \left(W_{\alpha'\alpha}J_{N,N-1}^\alpha c_N^\alpha + \delta_{\alpha'\alpha}c_{N-1}^\alpha\right)/\sqrt{k_\alpha}. \tag{51}$$

Using only the open-channel portion of R, the scattering matrix S and cross sections are given by

$$S_{\beta'\beta} = \sum_{\beta''=0}^{N_E-1}(1 + iR)_{\beta'\beta''}(1 - iR)_{\beta''\beta}^{-1}, \tag{52}$$

$$\sigma_{\beta'\beta} = \frac{\pi}{k_\beta^2}\frac{(2S+1)}{4}|S_{\beta'\beta} - \delta_{\beta'\beta}|^2. \tag{53}$$

C. Laguerre basis

One L^2-complete basis satisfying the JM requirements is the set of nonorthogonal Laguerre functions [2,26],

$$\phi_n(r) = x^{l+1}e^{-x/2}L_n^{2l+1}(x), \quad n = 0,1,\ldots,N-1, \tag{54}$$

where $x = \lambda r$, $l = 0$, and $L_n^\alpha(x)$ are the associated Laguerre polynomials [27], for example, $L_0^\alpha(x) = 1$ and

$L_1^\alpha(x) = -x + \alpha + 1$. The Laguerre polynomials could also be used to define an orthogonal basis:

$$R_n(r) = x^{l+1}e^{-x/2}L_n^{2l+2}(x), \quad n = 0,1,\ldots,N-1, \tag{55}$$

$$\int_0^\infty dr\ R_n(r)R_m(r) = \delta_{nm}C_n, \tag{56}$$

where $C_n = (n+2l+2)!/(\lambda n!)$. Since

$$L_n^{2l+2}(x) = \sum_{m=0}^{n} L_m^{2l+1}(x), \tag{57}$$

the set of $\{R_0(r), R_1(r), \ldots, R_{N_t-1}(r)\}$ covers identical functional L^2 subspace defined by $\{\phi_0(r), \phi_1(r), \ldots, \phi_{N_t-1}(r)\}$ and therefore were used as the starting basis for diagonalization of the target Hamiltonian (29) obtaining the target eigenvectors $\{|\chi_\alpha\rangle\}_{\alpha=0}^{N_t-1}$. When required, the liner expansion coefficients (30) were calculated numerically via

$$D_{nm} = \int_0^\infty dr\ \chi_n(r)\bar{\phi}_m(r), \tag{58}$$

where $\bar{\phi}_m(r)$ is the function biorthogonal to $\phi_n(r)$ [2,26],

$$\bar{\phi}_n(r) = \frac{n!}{(n+2l+1)!}\frac{\phi_n(r)}{r}, \tag{59}$$

$$\int_0^\infty dr\ \phi_n(r)\bar{\phi}_m(r) = \delta_{nm}. \tag{60}$$

The remaining $N - N_t$ basis functions are conveniently given by

$$\chi_n(r) = R_n(r)/\sqrt{C_n}, \quad N_t \leqslant n < N. \tag{61}$$

The final expressions for the reactance matrix require $J_{n,n-1}^\alpha$, s_n^α, and c_n^α, which are known exactly for this basis:

$$J_{n,n-1}^\alpha = \frac{n(n+1)q_\alpha}{2\sin\theta}, \tag{62}$$

$$c_n^\alpha + is_n^\alpha = -\frac{e^{-i(n+1)\theta}}{(n+1)}, \tag{63}$$

where only $l = 0$ is shown, $\cos\theta = (\eta^2 - \frac{1}{4})/(\eta^2 + \frac{1}{4})$, $\sin\theta = \eta/(\eta^2 + \frac{1}{4})$, $\eta = q_\alpha/\lambda$, and $q_\alpha = \sqrt{2(E - e_\alpha)}$ becomes complex for the closed channels.

D. Ionization

Bray and Stelbovics [28] demonstrated that correct total ionization cross section (TICS) could be calculated using only the L^2 description of atomic hydrogen. The TICS could be extracted from the channel cross sections by simply summing up the positive-energy target-state cross sections; that is,

$$\sigma_{\rm ion} \approx \sum_{\beta:e_\beta>0} \sigma_{\beta,0}, \tag{64}$$

where an atom is assumed to be in its ground state χ_0 before the collision with the electron. Note that Eq. (64) could be corrected by considering projection to the functional space of the exact bound target states [28], which speeds up the rate of convergence as a function of N_t. However, the correction is not applied to demonstrate that the JM method potentially could applied to other scattering problems where the exact target states may not be known.

Similar to the TICS, the single-differential ionization cross sections (SDCS) could be approximately extracted from the L^2 coupled-channel (CC) calculations without requiring the exact continuum target states [29]. The CC SDCS $d\sigma_{\rm CC}/d\varepsilon$ is calculated at the channel energy values via

$$\int_0^E d\varepsilon \frac{d\sigma_{ion}(\varepsilon)}{d\varepsilon} \approx \sum_{\beta:e_\beta>0} w_\beta \frac{d\sigma_{\rm CC}(e_\beta)}{d\varepsilon}, \tag{65}$$

$$d\sigma_{\rm CC}(e_\beta)/d\varepsilon = \sigma_{\beta,0}/w_\beta, \quad e_\beta > 0, \tag{66}$$

where the energy integration weights are given by

$$\begin{gathered} 0 < e_{\beta_c} < e_{\beta_c+1} < \cdots < e_{\beta_E-1} < e_{\beta_E} \leqslant E, \\ w_{\beta_c} = \frac{1}{2}(e_{\beta_c} + e_{\beta_c+1}), \\ w_\beta = \frac{1}{2}(e_{\beta+1} - e_{\beta-1}), \quad \beta_c < \beta < \beta_E \\ w_{\beta_E} = E - \frac{1}{2}(e_{\beta_E-1} + e_{\beta_E}), \\ \sum_{\beta=\beta_c}^{\beta_E} w_\beta = E, \end{gathered} \tag{67}$$

and where χ_{β_c} and χ_{β_E} are the *open* "continuum" target states with the lowest and largest positive energies, respectively.

The preceding SDCS integration weights can also be related to the close-coupling definition of the ionization amplitude [30] obtaining, in terms of Eq. (65),

$$\bar{w}_\beta = |\langle\psi_{e_\beta}|\chi_\beta\rangle|^{-2}, \tag{68}$$

where ψ_ε is the radial continuum Coulomb wave function satisfying

$$(H_t - \varepsilon)|\psi_\varepsilon\rangle = 0, \quad \langle\psi_\varepsilon|\psi_{\varepsilon'}\rangle = \delta(\varepsilon - \varepsilon'). \tag{69}$$

In Table I we show just how similar the two sets of weights are for a specified basis.

E. Radial grid

Even though the available computational resources continue to improve in cost, memory, and speed, the numerical optimization remains an important aspect of scattering problems [20,31]. In particular, the vector $\mathbf{r} = (r_1, r_2, \ldots, r_M)$ of equally spaced r grid points is quite wasteful when working with the exponentially vanishing JM Laguerre functions, where M is total number of the grid points, $r_j = (j-1)h_r$, and h_r is the radial step size, $j = 1,2,\ldots,M$. One possible optimization solution divides the considered radial space into regions in which h_r is increased based on how far the regions are from zero, for example, by doubling the step size [20]. This solution introduces extra adjustable parameters (e.g., number, position, and size of the regions), which are always undesirable from parsimonious considerations.

Another solution is the logarithmic grid (denoted LR, after "logarithm of r"),

$$y = \ln(r), \quad r(y) = \exp(y), \tag{70}$$

which was successfully used in the multiconfiguration Hartree-Fock (MCHF) calculations [32,33], where the equally spaced $\mathbf{r}$ grid is replaced with an equally spaced $\mathbf{y}$ grid,

TABLE I. SDCS energy integration weights for the Laguerre JM basis with $\lambda = 1$ and $N_t = 40$ (see text).

e_β	w_β	$\bar{w}_\beta$
0.003	0.003 99	0.003 99
0.007 35	0.004 74	0.004 73
0.012 48	0.005 56	0.005 54
0.018 47	0.006 47	0.006 45
0.025 42	0.007 51	0.007 48
0.033 48	0.008 71	0.008 67
0.042 83	0.010 1	0.010 06
0.053 68	0.011 74	0.011 69
0.066 32	0.013 7	0.013 64
0.081 09	0.016 06	0.015 98
0.098 44	0.018 94	0.018 83
0.118 96	0.022 48	0.022 33
0.143 41	0.026 91	0.026 71
0.172 78	0.032 52	0.032 26
0.208 45	0.039 75	0.039 39
0.252 28	0.049 23	0.048 71
0.306 92	0.061 92	0.061 16
0.376 12	0.079 3	0.078 17
0.465 52	0.103 77	0.102 01
0.583 67	0.139 37	0.136 51
0.744 26	0.193 24	0.188 34
0.970 15	0.278 8	0.269 88

$\mathbf{y} = (y_1, y_2, \ldots, y_{M_{\rm LR}})$. The LR grid dramatically improves efficiency of the numerical integration compared to the $\mathbf{r}$ grid by typically reducing the number of required grid points from $M = 701$ to $M_{\rm LR} = 201$. However some inconvenience remains: The r space must still be split into two regions by a small value $r_1 > 0$ obtaining the $(0,r_1)$ and (r_1,∞) regions, where only the latter is LR transformed [33].

In this study the LR grid was arguably improved by eliminating the inconvenience of the two regions in the LR transformation. This is achieved by "shifting" the LR grid by some constant c, where the resulting transformation was denoted LCR, after "logarithm of a constant plus r,"

$$x = \ln(c + r), \quad r(x) = \exp(x) - c. \tag{71}$$

The corresponding LCR wave functions and radial integration rules are found by starting from the kinetic energy radial integral,

$$K_{ij} = -\frac{1}{2}\int_0^\infty dr\ P_i(r)\left(\frac{d^2}{dr^2} - \frac{l(l+1)}{r^2}\right) P_j(r), \tag{72}$$

and defining the LCR transformation function $f(x)$ which converts the radial wave functions $P_i(r)$ to the corresponding LCR functions $F_i(x)$ via

$$P_i(r(x)) = f(x)F_i(x), \tag{73}$$

where r is now a function of x. If the considered functions $P_i(r)$ are orthonormal, their normalization is given by

$$\int_0^\infty dr\ P_i(r)P_j(r) = \delta_{ij}. \tag{74}$$

After substituting (73) into (72), for the radial equations in the new variable x to resemble one-dimensional motion (as for the r or LR's y coordinates), the term containing $dF(x)/dx$ must be eliminated arriving at

$$f(x) = \sqrt{c + r(x)}, \tag{75}$$

$$K_{ij} = -\frac{1}{2}\int_0^\infty dx\ F_i(x)\left(\frac{d^2}{dx^2} - \left[\frac{1}{4} + l(l+1)\frac{(c+r)^2}{r^2}\right]\right) F_j(x). \tag{76}$$

Other one-electron matrix elements of any operator $Q(r)$, for example, $Q(r) = V(r)$ or $Q(r) = 1$,

$$Q_{ij} = \int_0^\infty dr\ P_i(r)P_j(r)Q(r), \tag{77}$$

become

$$Q_{ij} = \int_0^\infty dx(c+r)^2 F_i(x)F_j(x)Q(r). \tag{78}$$

The LCR transformation is also consistent with the Hartree algorithm [34] of evaluating the so-called two-electron Slater integrals,

$$R^k(ab,a'b') = \int_0^\infty dr_1 \int_0^\infty dr_2 P_a(r_1)P_b(r_2) \times \frac{r_<^k}{r_>^{k+1}} P_{a'}(r_1)P_{b'}(r_2), \tag{79}$$

using differential equations, where $r_< = \min(r_1,r_2)$ and $r_> = \max(r_1,r_2)$. In the r space, the Hartree algorithm redefines $R^k(ab,a'b')$ as

$$R^k(ab,a'b') = \int_0^\infty P_a(r)P_{a'}(r)\frac{1}{r}Y^k_{bb'}(r)\,dr, \tag{80}$$

$$Y^k_{ab}(r) = Z^k_{ab}(r) + \int_r^\infty \left(\frac{r}{s}\right)^{k+1} P_a(s)P_b(s)\,ds, \tag{81}$$

$$Z^k_{ab}(r) = \int_0^r \left(\frac{s}{r}\right)^k P_a(s)P_b(s)\,ds \tag{82}$$

and numerically solves a pair of differential equations for Y^k and Z^k,

$$\frac{d}{dr}Z^k_{ab}(r) = P_a(r)P_b(r) - \frac{k}{r}Z^k_{ab}(r), \tag{83}$$

$$\frac{d}{dr}Y^k_{ab}(r) = \frac{1}{r}\left[(k+1)Y^k_{ab}(r) - (2k+1)Z^k_{ab}(r)\right], \tag{84}$$

with the boundary conditions $Z^k_{ab}(0) = 0$ and $Y^k_{ab}(r) \to Z^k_{ab}(r)$ as $r \to \infty$.

After the LR transformation the Hartree algorithm takes the form [33] of

$$\frac{d}{dy}\left[r^k Z^k_{ab}(y)\right] = r^{k+2}\bar{P}_a(y)\bar{P}_b(y), \tag{85}$$

$$\frac{d}{dy}\left[r^{-(k+1)}Y^k_{ab}(y)\right] = -(2k+1)r^{-(k+1)}Z^k_{ab}(y), \tag{86}$$

where $\bar{P}_a(y) = P_a(r)/\sqrt{r}$.

In the case of the LCR transformation, the same equations become

$$\frac{d}{dx}\left[r^k Z^k_{ab}(x)\right] = (c+r)^2 r^k F_a(x)F_b(x), \tag{87}$$

$$\frac{d}{dx}\left[r^{-(k+1)}Y^k_{ab}(x)\right] = -(2k+1)(c+r)r^{-(k+2)}Z^k_{ab}(x), \tag{88}$$

where the existing computer code for Y^k [35] needs to be only slightly modified without affecting the accuracy or stability of the numerical procedure.

And finally, the Numerov algorithm (e.g., [20]) could still be used via

$$\left\{\frac{d^2}{dx^2} - \frac{1}{4} + 2[E - V(r)](c+r)^2\right\} F(x) = 0 \qquad (89)$$

and was used to calculate the Coulomb continuum wave functions in this work.

III. RESULTS

All presented JM results were calculated on a consumer-grade laptop (2.2-GHz CPU, 3.5-GB RAM) with the SDCS calculations for $N_t = 90$ taking about four hours to complete at the three considered energies in Figs. 2 and 3, and it took about an extra hour to calculate all possible channel cross sections for the 501 energy points in Fig. 1.

The following typical parameter values were used: In all calculations $N = N_t + 1$ and $\ln(c) = -5$ for the LCR transformation; $r_{\max} = 250$, $M_{\rm LCR} = 901$ for $N_t = 30$; $r_{\max} = 500$, $M_{\rm LCR} = 1601$ for $N_t = 90$, where the radial grid was between zero and $r_{\max}$ and $M_{\rm LCR}$ is the number of equally spaced radial points in the LCR grid. The Laguerre basis exponential fall-off parameter λ was set to unity.

The agreement of the $N_t = 90$ results for the TICS with those of Jones and Stelbovics [20] is excellent (Fig. 1), indicating practical convergence with respect to the Laguerre basis size. We also plotted the results of a much smaller $N_t = 30$ calculation, which yields quite accurate results over most of the energy range. The discrepancies at the higher energies is due to the sparsity of high energy states in the smaller calculation. This could be improved by taking say $\lambda = 2$.

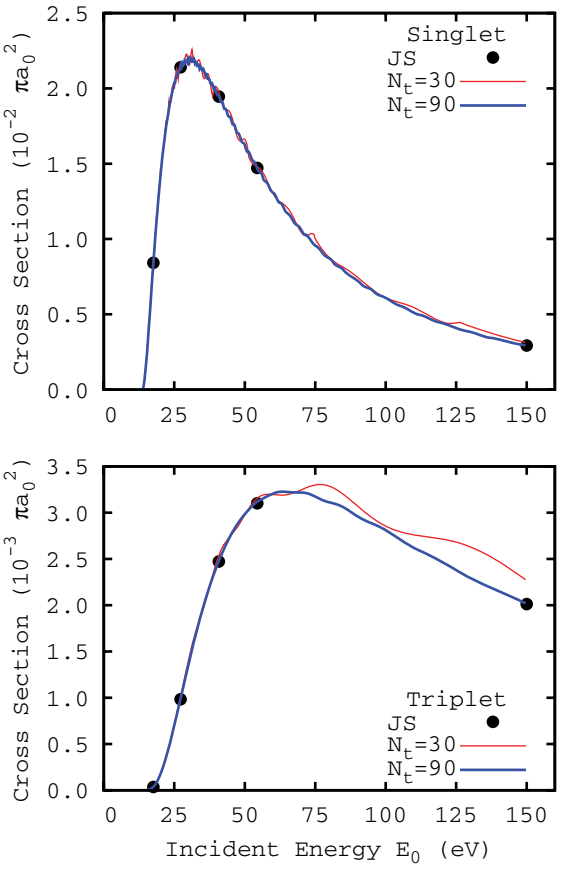

FIG. 1. (Color online) The singlet and triplet TICS (πa_0^2) in the Temkin-Poet model of e-H($1s$) scattering. The JS results are by Jones and Stelbovics [20]. The spin weights have been included in the cross sections. The JM calculations are denoted by N_t, where $N = N_t + 1$ (see text).

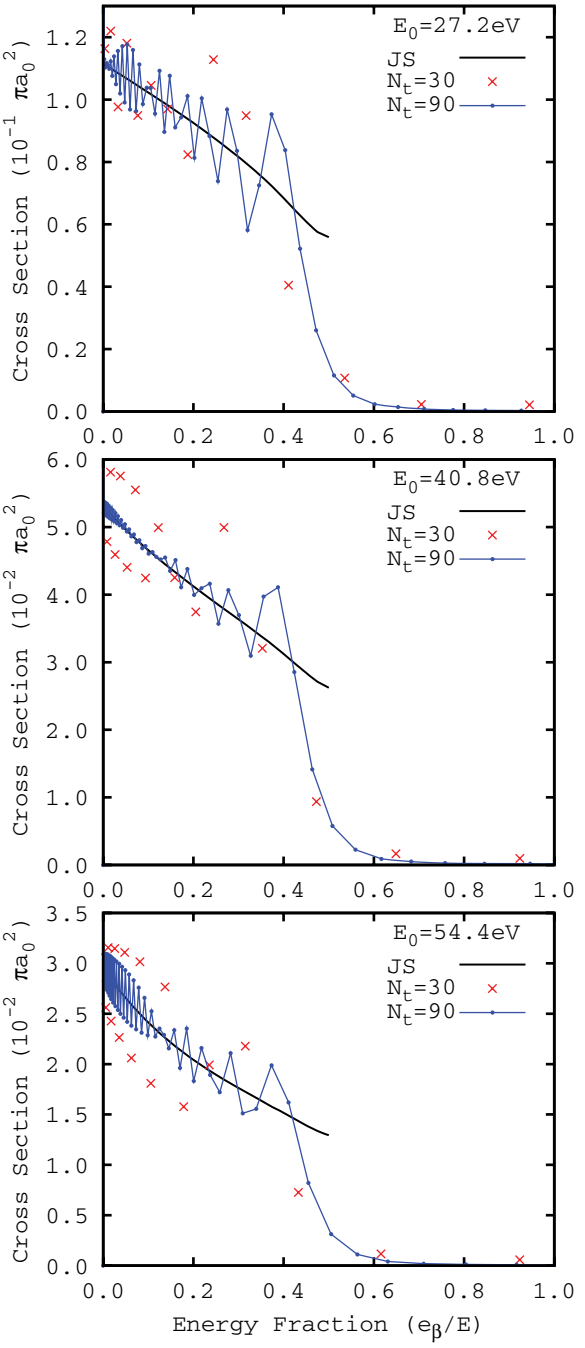

FIG. 2. (Color online) Same as in Fig. 1 but for the singlet SDCSs (πa_0^2/Hartree) vs energy fraction e_β/E for the impact energies (E_0) shown. The $N_t = 90$ points have been connected with straight lines to help guide the eye.

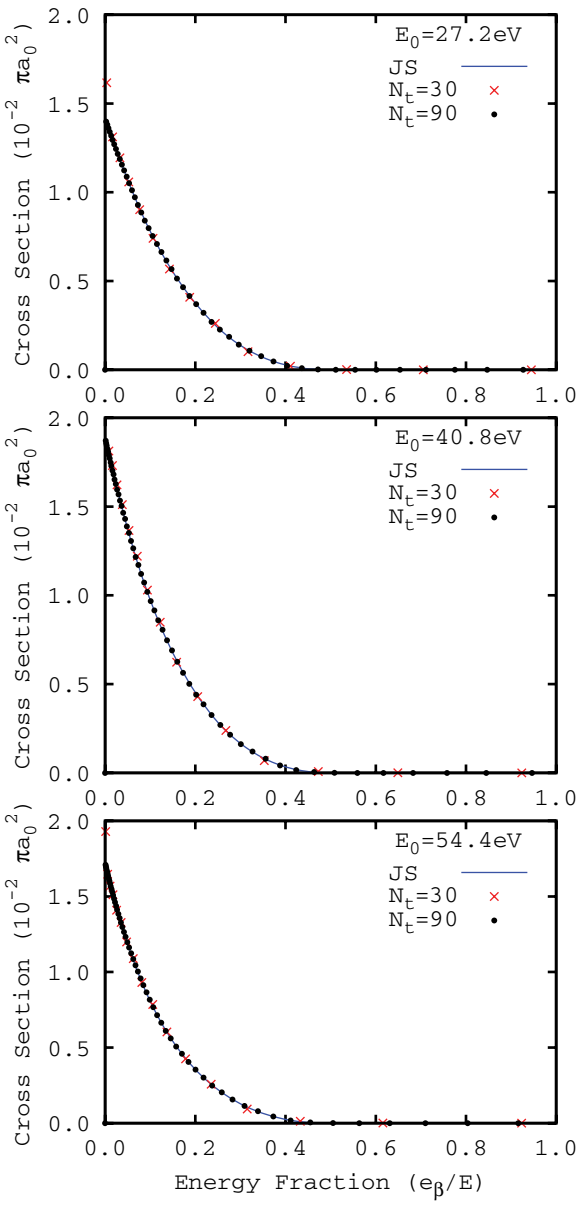

FIG. 3. (Color online) Same as in Fig. 2 but for the triplet SDCS.

Having performed very many calculations (not presented), it is clear that the larger bases yield accurate results over broader energy ranges with less dependence on variation of λ.

Having demonstrated that the JM method yields correct TICSs, we next turn to examining the single-differential cross sections (SDCSs). The SDCSs give an estimate of the cross section for an electron ejected at a specified energy. In experiment, and theories that treat the two electrons on an equal footing, the SDCS is symmetric about $E/2$. Then the TICS is obtained by integrating from 0 to $E/2$. However, in Figs. 2 and 3 it is clear that the JM estimates of the SDCS are not symmetric about $E/2$ (energy fraction equals 0.5). Instead, they behave in the same way as the CCC-calculated SDCS [36] and for the same reason. In close-coupling methods such as the JM, the TICS is obtained from all open states. This is the origin of Eq. (65). As suggested by Stelbovics [37], the Laguerre-basis expansion is behaving like a Fourier expansion of a step function, with the step being at $E/2$. If the size of the step is finite, as it is in the singlet case presented in Fig. 2, then the JM results oscillate about the true result, with convergence at $E/2$ to one quarter (underlying amplitude to a half as in Gibbs phenomenon) of the true result. If the step has zero height, then the underlying results are smooth and readily convergent (Fig. 3).

It is important to appreciate that the basis sizes presented in Fig. 2 are the largest yet undertaken utilizing a close-coupling method. This is arguably the most direct support so far for Stelbovics's interpretation [37] of the coupled-L^2-channels SDCS. The larger bases generally show smaller oscillation amplitude compared to the bases with a smaller N_t, as might be expected. Performing such large calculations within the CCC method, for example, is not practical due to computational constraints.

IV. CONCLUSIONS

We have implemented a highly numerically efficient and stable implementation of the J-matrix approach to electron-atom scattering. We have found that very large Laguerre bases may be implemented and the convergence is to the correct results. The underlying ionization scattering amplitudes behave in the same way as in the CCC method. However, unlike the CCC method the results are available on a broad range of incident energies after a single diagonalization of the two-electron Hamiltonian, just like in the R-matrix method. A further strength of the method is that the total wave function may be reconstructed in an L^2 form, while retaining channel information. We hope to use this fact in the future to apply the method to ionization-plus-excitation processes, for example, in e-He collisions [31].

ACKNOWLEDGMENTS

The authors thank Ron White, Ian Whittingham, and Bruce Litow for helpful discussions. This work was supported by the Australian Research Council.

[1] E. J. Heller and H. A. Yamani, Phys. Rev. A **9**, 1201 (1974).
[2] J. Broad and W. Reinhardt, J. Phys. B **9**, 1491 (1976).
[3] E. J. Heller and H. A. Yamani, Phys. Rev. A **9**, 1209 (1974).
[4] I. Bray, D. A. Konovalov, and I. E. McCarthy, Phys. Rev. A **43**, 1301 (1991).
[5] I. Bray and A. T. Stelbovics, Phys. Rev. A **46**, 6995 (1992).
[6] D. A. Konovalov and I. E. McCarthy, J. Phys. B **27**, L741 (1994).
[7] D. A. Konovalov and I. E. McCarthy, J. Phys. B **27**, L407 (1994).
[8] D. A. Konovalov and I. E. McCarthy, J. Phys. B **28**, L139 (1995).
[9] I. Bray, I. McCarthy, and A. T. Stelbovics, J. Phys. B **29**, L245 (1996).
[10] B. R. Odgers, M. P. Scott, and P. G. Burke, J. Phys. B **29**, 4320 (1996).
[11] S. A. Zaytsev, V. A. Knyr, Y. V. Popov, and A. Lahmam-Bennani, Phys. Rev. A **75**, 022718 (2007).

[12] S. A. Zaytsev, Phys. Rev. A **76**, 062706 (2007).
[13] A. D. Alhaidari, H. Bahlouli, M. S. Abdelmonem, F. Al Ameen, and T. Al Abdulaal, Phys. Lett. A **364**, 372 (2007).
[14] W. Vanroose, J. Broeckhove, and F. Arickx, Phys. Rev. Lett. **88**, 010404 (2001).
[15] H. A. Yamani, A. D. Alhaidari, and M. S. Abdelmonem, Phys. Rev. A **64**, 042703 (2001).
[16] A. D. Alhaidari, H. A. Yamani, and M. S. Abdelmonem, Phys. Rev. A **63**, 062708 (2001).
[17] P. Horodecki, Phys. Rev. A **62**, 052716 (2000).
[18] A. Temkin, Phys. Rev. **126**, 130 (1962).
[19] R. Poet, J. Phys. B **11**, 3081 (1978).
[20] S. Jones and A. T. Stelbovics, Phys. Rev. A **66**, 032717 (2002).
[21] S. Jones and A. T. Stelbovics, Phys. Rev. Lett. **84**, 1878 (2000).
[22] M. Baertschy, T. N. Rescigno, W. A. Isaacs, and C. W. McCurdy, Phys. Rev. A **60**, R13 (1999).
[23] I. Bray and A. T. Stelbovics, Phys. Rev. Lett. **69**, 53 (1992).
[24] L. D. Landau and E. M. Lifshitz, *Quantum Mechanics (Non-relativistic Theory)* (Pergamon Press, Oxford, UK, 1985), Vol. 3 of Course of Theoretical Physics, 3rd ed.
[25] J. R. Taylor, *Scattering Theory* (Wiley & Sons, New York, 1972).
[26] H. A. Yamani and L. Fishman, J. Math. Phys. **16**, 410 (1975).
[27] M. Abramowitz and I. A. Stegun (Eds.), *Handbook of Mathematical Functions* (Dover Publications, Mineola, NY, 1965).
[28] I. Bray and A. T. Stelbovics, Phys. Rev. Lett. **70**, 746 (1993).
[29] D. A. Konovalov, I. Bray, and I. E. McCarthy, J. Phys. B **27**, L413 (1994).
[30] I. Bray, Phys. Rev. Lett. **89**, 273201 (2002).
[31] P. L. Bartlett and A. T. Stelbovics, Phys. Rev. A **81**, 022715 (2010).
[32] O. Jitrik and C. F. Bunge, Phys. Rev. A **56**, 2614 (1997).
[33] C. Froese Fischer, T. Brage, and P. Jonsson, *Computational Atomic Structure* (Institute of Physics Publishing, London, 1997).
[34] D. R. Hartree, *The Calculation of Atomic Structures* (Wiley, New York, 1957).
[35] C. Froese Fischer, Comput. Phys. Commun. **43**, 355 (1987).
[36] I. Bray, Phys. Rev. Lett. **78**, 4721 (1997).
[37] A. T. Stelbovics, Phys. Rev. Lett. **83**, 1570 (1999).